PI3K/Akt signaling requires spatial compartmentalization in plasma membrane microdomains

Xinxin Gao[a], Pamela R. Lowry[a], Xin Zhou[a], Charlene Depry[a], Zhikui Wei[b], G. William Wong[b], and Jin Zhang[a,c,d,1]

Departments of [a]Pharmacology and Molecular Sciences, [b]Physiology and Center for Metabolism and Obesity Research, and [c]Oncology, and [d]The Solomon H. Snyder Department of Neuroscience, The Johns Hopkins University School of Medicine, Baltimore, MD 21205

Edited* by Lewis C. Cantley, Beth Israel Deaconess Medical Center, Boston, MA, and approved July 25, 2011 (received for review December 23, 2010)

Spatial compartmentalization of signaling pathway components generally defines the specificity and enhances the efficiency of signal transduction. The phosphatidylinositol 3-kinase (PI3K)/Akt pathway is known to be compartmentalized within plasma membrane microdomains; however, the underlying mechanisms and functional impact of this compartmentalization are not well understood. Here, we show that phosphoinositide-dependent kinase 1 is activated in membrane rafts in response to growth factors, whereas the negative regulator of the pathway, phosphatase and tensin homolog deleted on chromosome 10 (PTEN), is primarily localized in nonraft regions. Alteration of this compartmentalization, either by genetic targeting or ceramide-induced recruitment of PTEN to rafts, abolishes the activity of the entire pathway. These findings reveal critical steps in raft-mediated PI3K/Akt activation and demonstrate the essential role of membrane microdomain compartmentalization in enabling PI3K/Akt signaling. They further suggest that dysregulation of this compartmentalization may underlie pathological complications such as insulin resistance.

biosensor | FRET | fluorescence imaging

Phosphatidylinositol 3-kinase (PI3K)/Akt signaling plays a major role in cell metabolism, growth, and apoptosis (1). Defects in PI3K/Akt signaling have been implicated in many diseases, including cancer (2) and type 2 diabetes (3). The activation of this pathway is initiated at the plasma membrane, where phosphatidylinositol (3,4,5) trisphosphate [PI(3,4,5)P_3], generated by PI3K and degraded by phosphatase and tensin homolog deleted on chromosome 10 (PTEN), recruits Akt to the membrane. Once at the membrane, Akt is phosphorylated in its activation loop by phosphoinositide-dependent kinase 1 (PDK1) and on its hydrophobic motif by mammalian TOR complex 2 (4). After these two phosphorylation events, Akt adopts an active conformation and proceeds to phosphorylate a variety of protein substrates involved in diverse cellular processes. Although the activation of the PI3K/Akt signaling pathway has been extensively studied, the mechanisms by which several critical steps are regulated in the cell are still not well understood (5). For instance, it remains unclear whether growth factor stimulation leads to activation of PDK1. A better understanding of the complex cellular regulation of PI3K/Akt signaling may require dissecting these molecular events in their specific cellular contexts.

Given that the plasma membrane is the site of activation for the PI3K/Akt pathway, it is no surprise that plasma membrane microdomains, such as sphingolipid- and cholesterol-enriched membrane rafts (6), emerge as important regulators of this pathway. A recent study using fluorescence correlation spectroscopy has indicated that raft microdomains play important roles in recruiting Akt to the membrane after PI(3,4,5)P_3 production (7). Disruption of membrane rafts was shown to inhibit the recruitment process (7). In addition, we have observed a preferential activation of Akt in membrane rafts by using a fluorescence resonance energy transfer (FRET)-based Akt activity reporter (AktAR) (8). However, the molecular mechanisms by which membrane rafts control Akt recruitment and regulate its activation are yet to be determined. Furthermore, although spatial compartmentalization is believed to be a key mechanism for achieving specificity and efficiency in general (9), the role of membrane microdomain compartmentalization in PI3K/Akt signaling remains poorly defined.

To address these questions, we used genetic targeting as a general strategy, directing either a fluorescent biosensor or an active enzyme to specific plasma membrane microdomains. The use of targeted biosensors made it possible to monitor the same molecular process in different cellular contexts, and genetic targeting of an active form of a negative regulator allowed perturbation of a signaling event in specific membrane microdomains, thereby testing the functional importance of microdomain-specific signaling. Using this strategy, we investigated the membrane compartmentalization of the signaling molecules dictating Akt activation. We demonstrated that PDK1 can be activated in response to growth factors and that this activation occurs in membrane rafts. Furthermore, we found that PTEN is localized outside of membrane rafts and that relocalizing it to rafts, instead of affecting the specificity and efficiency of the signaling response, abolished the activity of the entire pathway.

Results

PDK1 Is Activated in Membrane Rafts. The PDK1-mediated phosphorylation of the activation loop of Akt is required for Akt activity. Although the importance of PDK1 in the PI3K/Akt pathway has been established, the regulation of PDK1 remains controversial (5). It has been suggested that PDK1 is constitutively active throughout the cell and cannot be further activated by growth factor stimulation (10). However, based on the observation that pervanadate (PV) can increase PDK1 activity at the plasma membrane, it has been suggested that PDK1 can be activated by growth factor stimulation in a similar, spatially controlled fashion (11). Thus, whether and how PDK1 is regulated by growth factors remains controversial.

To address this problem, we set out to analyze the activation of PDK1 in its native cellular context, the plasma membrane of living cells. More specifically, we wanted to examine different plasma membrane microdomains by generating a FRET-based PDK1 activation reporter (PARE) that could be targeted to these microdomains. To this end, we generated a construct in which the full-length PDK1 was sandwiched between a pair of fluorescent proteins, enhanced cyan fluorescent protein (ECFP)

Author contributions: X.G., Z.W., G.W.W., and J.Z. designed research; X.G., P.R.L., X.Z., C.D., and Z.W. performed research; X.G., P.R.L., X.Z., C.D., Z.W., and J.Z. analyzed data; and X.G. and J.Z. wrote the paper.

The authors declare no conflict of interest.

*This Direct Submission article had a prearranged editor.

[1]To whom correspondence should be addressed. E-mail: jzhang32@jhmi.edu.

This article contains supporting information online at www.pnas.org/lookup/suppl/doi:10.1073/pnas.1019386108/-/DCSupplemental.

and citrine (Fig. 1*A*), to allow us to monitor the conformational changes in PDK1 during its activation by changes in FRET. This reporter was targeted to membrane rafts by using a targeting motif derived from Lyn kinase, and to nonraft regions of the plasma membrane by using a targeting motif derived from K-ras (8) (Fig. 1*A*). Sucrose density gradient fractionation experiments confirmed the localization of the two plasma membrane-targeted PDK1 reporters to the desired microdomains (Fig. 1*B*).

We then used these PDK1 activation reporters to examine the conformational changes associated with PV-induced activation of PDK1 in serum-starved NIH 3T3 cells. No emission ratio change was observed in cells expressing the untargeted reporter, which also did not translocate effectively to the plasma membrane. However, we saw a striking difference between the raft-targeted and nonraft-targeted PDK1 reporters: Only the raft-targeted PDK1 reporter showed an increase (of 20.7 ± 3.3%; n = 5) in the yellow-to-cyan emission ratio (Fig. 1*C* and Fig. S1), suggesting that the PV-induced activation of PDK1 (Fig. S2), which was reported to occur at the plasma membrane, instead occurs primarily in raft microdomains of the plasma membrane.

We next examined growth factor-induced PDK1 activation. Serum-starved NIH 3T3 cells expressing one of the three variants of the PDK1 reporter were treated with 50 ng/mL platelet-derived growth factor (PDGF) and imaged. Strikingly, the raft-targeted PDK1 reporter showed an increase of 19 ± 4% (n = 7) in the yellow-to-cyan emission ratio upon growth factor stimulation, whereas no emission ratio change was observed in cells expressing the untargeted or nonraft-targeted PDK1 reporter (Fig. 1 *D–F*). Importantly, raft disruption using methyl-β-cyclodextrin (MCD) also abolished the response of the raft-targeted PDK1 activation reporter to 50 ng/mL PDGF (Fig. S3) but did not affect the response of a nonraft-targeted Akt activity reporter (8). These data suggest that growth factor stimulation can induce the activation of PDK1 and that this activation also occurs primarily in the raft microdomains of the plasma membrane.

Using the raft-targeted PDK1 reporter, we also examined the ability of other growth factors to activate PDK1 in live cells. Stimulation of serum-starved HeLa cells with 100 ng/mL epidermal growth factor (EGF) induced an emission ratio increase in the case of the raft-targeted PDK1 reporter (Fig. S4*A*). As was true for PDGF stimulation, the EGF-induced response was also restricted to the membrane raft microdomains (Fig. S4*A*), indicating that the differential activation pattern of PDK1 in the plasma membrane microdomains was not unique to NIH 3T3 cells or PDGF receptor activation.

PDK1, like Akt, possesses a pleckstrin homology (PH) domain that binds to 3′-phosphoinositides, including PI(3,4,5)P_3 and PI(3,4)P_2. Studies have demonstrated that the phosphoinositide binding of PDK1 plays a crucial role in controlling the activation of Akt and its downstream signaling. For instance, PDK1$^{K465E/K465E}$ knock-in mice expressing a mutant PDK1 that is incapable of binding to 3′-phosphoinositides are known to exhibit impaired growth and a marked insulin resistance and glucose intolerance (12). We therefore asked whether the observed PDK1 activation in response to PV or PDGF depended on its binding to 3′-phosphoinositides. As shown in Fig. S4 *B* and *C*, mutation of the two Arg residues (R472/474) responsible for phosphoinositide binding to Ala (13) abolished PDK1 activation, as indicated by a lack of response from the raft-targeted PDK1 reporter variant. Furthermore, addition of the PI3K inhibitor LY294002 caused a reversal of the response of Lyn-PARE after the PDGF-, EGF- or PV-stimulated emission ratio change was stabilized (Fig. S4), indicating that the response of the raft-targeted PDK1 reporter is reversible and depends on PI3K activity.

The lack of change in the nonraft regions may reflect the inefficient activation of PDK1 in these regions. Alternatively, PDK1 may be locked into conformations that correspond to high PDK1 activity in these membrane microdomains. To directly examine endogenous PDK1 activity in these specific microdomains, we studied the phosphorylation of the natural substrate of PDK1, Akt, in raft and nonraft regions by sucrose density gradient separation followed by Western blot analysis. Phosphorylation of Akt by PDK1 at T308 was found to occur preferentially in the membrane rafts of insulin-stimulated HEK 293 cells, with 5.0 ± 2.5-fold stronger phosphoAkt signal (normalized to the total Akt signal) in raft fractions than in nonraft fractions (Fig. S5 *A* and *B*). This finding suggests that PDK1 is preferentially activated in membrane rafts. At the same time, it appears that some basal activity of PDK1 is present in nonraft microdomains (Fig. S5*C*). The Thr308 phosphorylation observed in the nonraft fractions could be due to the basal activity of PDK1 and/or some diffusion and redistribution of phosphorylated Akt between membrane microdomains. In fact, considering the diffusion of activated PDK1 between membrane compartments, this fivefold difference is likely an underestimation. Taken together, these studies suggest that PDK1 can be activated by a variety of stimulating signals, and this activation occurs in the raft microdomains of the plasma membrane.

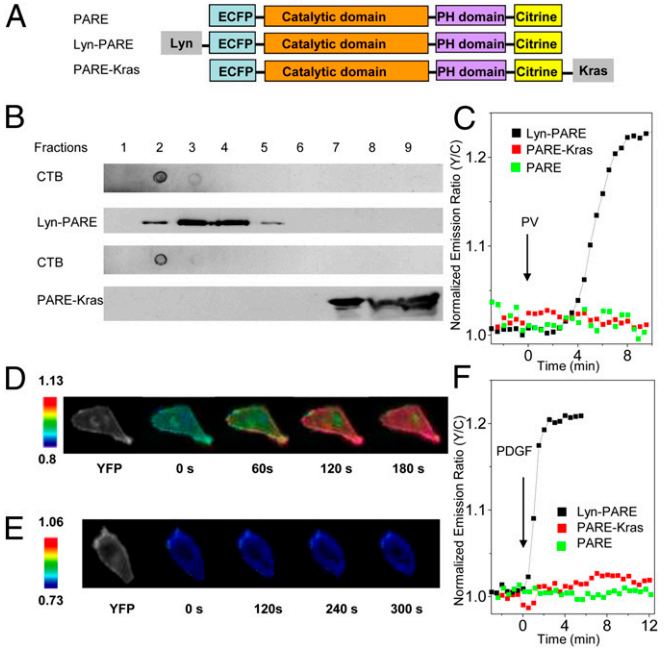

Fig. 1. Development and characterization of PDK1 activation reporters. (*A*) The PDK1 activation reporter PARE was generated with full-length PDK1 sandwiched by a pair of fluorescent proteins, ECFP and citrine. PARE was targeted to membrane rafts by using a targeting motif derived from Lyn kinase and to nonraft regions of the plasma membrane by using a targeting motif derived from Kras. (*B*) The localization of Lyn-PARE and PARE-Kras was confirmed by sucrose density gradient fractionation. Total cell lysates from HEK 293 cells overexpressing Lyn-PARE or PARE-Kras were subjected to sucrose density gradient fractionation, followed by Western blotting. Cholera toxin subunit B (CTB) was used as a raft marker. The reporters were detected with an anti-GFP antibody. (*C*) Representative time courses showing the responses of PARE (n = 5), Lyn-PARE (n = 5), and PARE-Kras (n = 4) in serum-starved NIH 3T3 cells after stimulation with 100 μM PV. (*D*) Pseudocolor images showing the response of Lyn-PARE to 50 ng/mL PDGF in NIH 3T3 cells. The yellow fluorescence image (*Left*) shows the localization of Lyn-PARE. (*E*) Pseudocolor images showing the null response of PARE-Kras to 50 ng/mL PDGF in NIH 3T3 cells. The yellow fluorescence image (*Left*) shows the localization of PARE-Kras. (*F*) Stimulation of serum-starved NIH 3T3 cells with 50 ng/mL PDGF induced an emission ratio change in Lyn-PARE (n = 7), but not PARE (n = 5) or PARE-Kras (n = 6).

Localization of PTEN to Nonraft Regions of the Plasma Membrane Is Important for Proper Akt Signaling. We have shown that Akt activation, which depends on accumulation of 3′-phosphoinositides, is faster and stronger in membrane rafts (8). Our further demonstration of raft-specific activation of PDK1, also downstream of 3′-phosphoinositides, prompted us to examine the regulation of 3′-phosphoinositides in the context of plasma membrane microdomains. As a lipid phosphatase, PTEN plays an important role in restricting the accumulation of 3′-phosphoinositides. It has been shown to be largely cytosolic, with a small variable proportion associated with the plasma membrane (14). Although membrane-associated PTEN is the actual species that catalyzes the degradation of 3′-phosphoinositides, its microdomain-specific membrane association and the importance of this membrane compartmentalization are not well understood.

We first examined the membrane localization of endogenous PTEN by sucrose density gradient fractionation of crude plasma membranes isolated from HEK 293 cells. The majority of the membrane PTEN was found to reside in nonraft regions, with only a small amount being present in the membrane rafts (Fig. 2 *A* and *B*). The same pattern was also observed in 3T3-L1 adipocytes (Fig. 3*A*). These results indicated that PTEN primarily resides in the nonraft regions of the plasma membrane, consistent with previous observations (15, 16).

We then used a genetic targeting approach to determine the role of membrane microdomain compartmentalization of PTEN in controlling downstream signaling. An active form of PTEN, PTEN A4 (17), has been described. In this form, four residues of the C-terminal tail region have been mutated to Ala to abolish the inhibitory phosphorylation. To alter the membrane microdomain localization of PTEN, we targeted PTEN A4 to raft microdomains with the Lyn motif (Fig. 2*C*). As a control, a nonraft-targeted PTEN was also generated by attaching the Kras motif to PTEN A4 (Fig. 2*C*). The membrane localization of Lyn-PTEN A4 and PTEN A4-Kras was verified by sucrose density gradient fractionation (Fig. 2*D*).

The effects of perturbing the membrane microdomain localization of PTEN were assessed at the levels of PDK1 activation, Akt recruitment, and Akt activity by using a series of fluorescent biosensors. First, we found that targeting of the active PTEN to membrane rafts via Lyn-PTEN A4 prevented growth factor-induced PDK1 activation, because no emission ratio change was observed in growth factor-stimulated NIH 3T3 cells coexpressing properly localized Lyn-PTEN A4 and the Lyn-PDK1 reporter (Fig. 2*E*). The presence of PTEN A4-Kras, however, did not prevent the activation of PDK1 in membrane rafts, although it reduced the response of Lyn-PARE (Fig. 2*E* and Fig. S6). The response to PDGF could be restored by treatment with 50 mM H_2O_2, a condition that has been shown to inhibit cellular PTEN (18) (Fig. S6*A*). This result further indicates that the suppression of raft PDK1 activation is caused by the high PTEN activity.

The strong inhibitory effect of Lyn-PTEN A4 on PDK1 activation could also be seen at the level of the membrane recruitment of Akt, as indicated by the lack of plasma membrane translocation of the YFP-tagged PH domain of Akt in response to growth factor stimulation (Fig. 2*F*). Inhibition of PTEN activity with 50 mM H_2O_2 restored the membrane translocation (Fig. S7*A*). In contrast, active PTEN targeted to nonraft regions had a much lower inhibitory effect, producing a 40% reduction in Akt-PH translocation compared with cells lacking PTEN A4 expression (Fig. S7*B*). This nonspecific effect, presumably a result of the overexpression of an active PTEN, could also be reversed by H_2O_2 treatment (Fig. S7).

Finally, we used a developed FRET-based Akt activity reporter, AktAR (8), to probe the effect of perturbing membrane microdomain localization of PTEN on growth factor-stimulated Akt activity. This biosensor serves as a surrogate substrate for Akt and reports Akt activity by phosphorylation-dependent

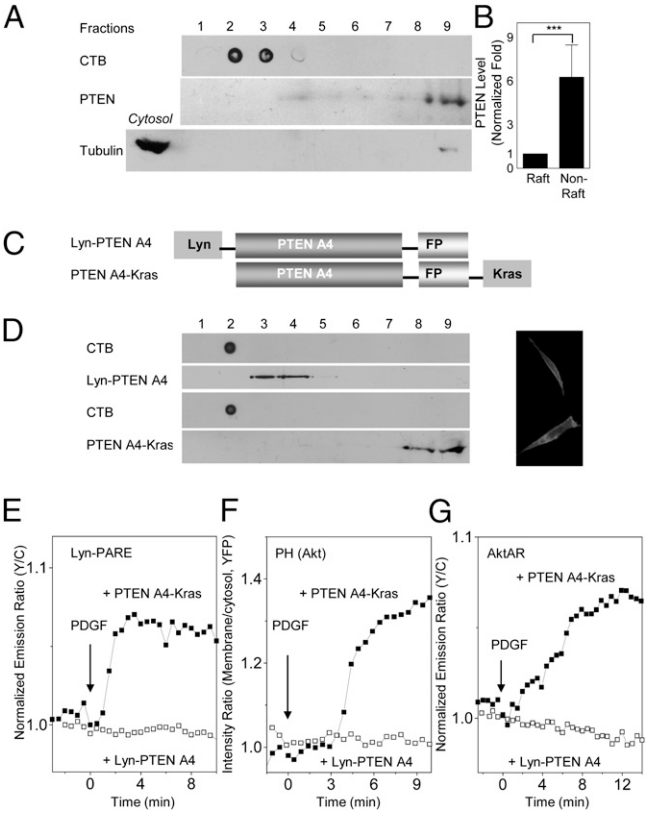

Fig. 2. Genetic targeting of PTEN to membrane rafts abolishes PDK1 activation, Akt membrane recruitment, and Akt activity. (*A*) PTEN is primarily localized to nonraft regions of the plasma membrane. Crude plasma membranes from HEK 293 cells were solubilized and subjected to sucrose density gradient fractionation, followed by Western blotting with an anti-PTEN antibody. CTB was used as a raft marker. Anti-tubulin was used to ensure the separation of membrane proteins from cytosolic proteins. (*B*) Statistically significant differences between PTEN levels in rafts and nonraft regions (***$P < 0.001$; $n = 3$). Densitometric analysis indicated that the majority of the membrane PTEN resides in nonraft regions. (*C*) PTEN A4, fused with a C-terminal fluorescent protein (FP), was targeted to membrane rafts and nonraft regions with a Lyn or Kras motif. (*D*) The membrane localization of Lyn-PTEN A4 or PTEN A4-Kras was verified by sucrose density gradient fractionation of total cell lysates of HEK 293 cells expressing Lyn-PTEN A4-YFP or PTEN A4-YFP-Kras. CTB was used as a raft marker. Targeted PTEN A4 was detected with an anti-GFP antibody. Yellow fluorescence images show the membrane localization of PTEN. (*E*) Representative time courses indicating that the response of Lyn-PARE was abolished by Lyn-PTEN A4 ($n = 5$; PTEN fused with mCherry), but not PTEN A4-Kras ($n = 7$). (*F*) Representative time courses demonstrating that the membrane translocation of the Akt PH domain was abolished by Lyn-PTEN A4 ($n = 4$; PTEN fused with mCherry), but not PTEN A4-Kras ($n = 4$). (*G*) Representative time courses indicating that the response of AktAR was abolished by Lyn-PTEN A4 ($n = 7$; PTEN fused with mCherry), but not PTEN A4-Kras ($n = 6$).

increases in FRET. As shown in Fig. 2*G*, the presence of Lyn-PTEN A4 abolished the response of AktAR to PDGF stimulation in NIH 3T3 cells, whereas cells expressing PTEN A4-Kras were still able to respond to PDGF stimulation (Fig. 2*G* and Fig. S8). These data demonstrate that preferential localization of PTEN outside membrane rafts has an important functional consequence for maintaining PDK1 and Akt activity, and mislocalizing it to raft microdomains abolished downstream signaling.

Given the importance of the specific membrane microdomain localization of PTEN in maintaining the activity of the PI3K/Akt pathway, we postulated that dysregulation of this compartmentalization can disrupt cellular functions and contribute to the development of pathologic conditions. Ceramide, a sphingolipid

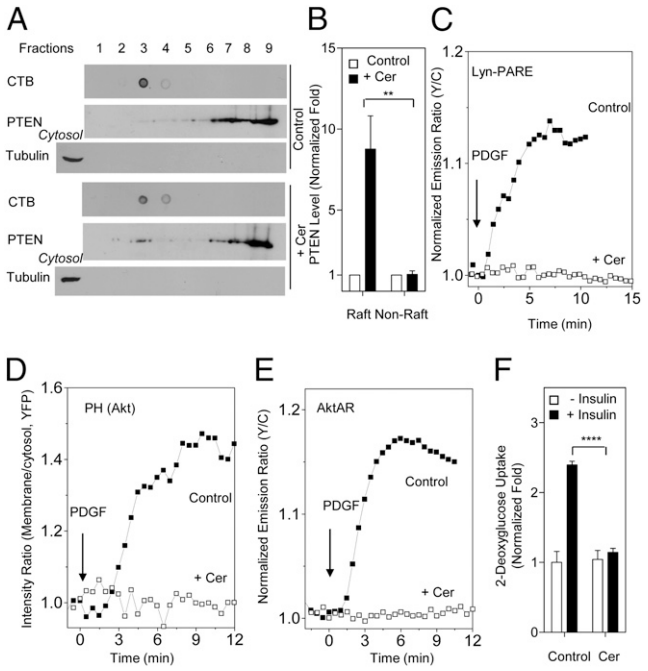

Fig. 3. Ceramide recruits PTEN to membrane rafts and suppresses PDK1 activation, Akt membrane recruitment, and Akt activity. (*A*) Ceramide recruits PTEN to membrane rafts. Crude plasma membranes from 3T3 L1 adipocytes (in the presence or absence of 50 μM C_2-ceramide) were solubilized and subjected to sucrose density gradient fractionation, followed by Western blotting with an anti-PTEN antibody. CTB was used as a raft marker. Anti-tubulin was used to ensure the separation of membrane proteins from cytosolic proteins. (*B*) Densitometric analysis indicated a statistically significant difference between the raft PTEN levels in the presence of C_2-ceramide and those in its absence (**$P < 0.01$; $n = 3$). (*C*) Representative time courses showing that the response of Lyn-PARE ($n = 7$) in 3T3 L1 preadipocytes was abolished by preincubation with 50 μM C_2-ceramide ($n = 6$). (*D*) Representative time courses showing that membrane translocation of Akt PH domain ($n = 3$) in 3T3 L1 preadipocytes was abolished by preincubation with 50 μM C_2-ceramide ($n = 3$). (*E*) Representative time courses showing that the response of AktAR ($n = 6$) in 3T3 L1 preadipocytes was abolished by preincubation of 50 μM C_2-ceramide ($n = 5$). (*F*) Ceramide-mediated suppression of insulin-induced glucose uptake in 3T3 L1 adipocytes. Preincubation of 50 μM C_2-ceramide with 3T3 L1 adipocytes for 60 min inhibited insulin-induced glucose uptake in these cells (****$P < 0.0001$; $n = 3$).

that is known to antagonize insulin action, has been suggested to be an important contributor to insulin resistance (19). The underlying mechanism is not clearly understood, but the major effect appears to be the inhibition of the PI3K/Akt pathway. Interestingly, raft disruption achieved through inhibition of ceramide synthesis also inhibited Akt signaling (7), suggesting that both up- and down- regulation of physiological levels of ceramide could lead to Akt inhibition. Recently, ceramide treatment was shown to translocate PTEN to caveolin-enriched microdomains in certain cell lines (20, 21). We confirmed this finding by showing that preincubation of 3T3-L1 adipocytes with C_2-ceramide, a cell-permeable ceramide analog, greatly increased the amount of PTEN found in raft fractions (8.8 ± 2.1-fold; $n = 3$) (Fig. 3 *A* and *B* and Fig. S9). Importantly, treatment with C_2-ceramide also blocked the PDGF-induced activation of PDK1 in membrane rafts and membrane recruitment of Akt, and Akt activity, in 3T3 L1 preadipocytes and NIH 3T3 cells (Fig. 3 *C–E*, Fig. S10, and Fig. S11). These findings are most consistent with a model in which ceramide suppresses PDK1 and Akt activity by specifically recruiting PTEN to membrane rafts. Furthermore, in agreement with previous reports (22), we found that this treatment also blocked insulin-induced glucose uptake in 3T3 L1 adipocytes (Fig. 3*F*), an important function mediated by the PI3K/Akt pathway, suggesting that ceramide-induced mislocalization of PTEN to membrane rafts can inhibit the functional output of the PI3K/Akt pathway.

Discussion

Activation of the PI3K/Akt pathway involves a series of tightly coupled molecular events occurring at the plasma membrane. However, how these molecular events are organized in the local signaling microdomains is not clear. By using a genetic targeting strategy in which the signaling events in specific membrane microdomains were monitored or perturbed, we have demonstrated that raft microdomains are critical for organizing the localization of active positive and negative regulators of the pathway. Dysregulation of this membrane compartmentalization undermined PI3K/Akt signaling transduction and may underlie pathological complications such as insulin resistance.

As the kinase controlling the activation loop phosphorylation of Akt, PDK1 plays a critical role in PI3K/Akt signaling. Despite advances (23), the activation mechanisms of PDK1 are still not well understood. Here, in contrast to the previously held belief that PDK1 is constitutively active and cannot be further activated by growth factor stimulation (10), we show that PDK1 can be activated by various growth factors, and this induced activation occurs in membrane rafts. Our genetic targeting approach allowed us to focus on specific events in specific plasma membrane domains of living cells, thereby enhancing the sensitivity of the assay and revealing previously unrecognized mechanistic details. This pool of further-activated PDK1 may directly contribute to the preferential activation of Akt in membrane rafts (8) and the proper functioning of the pathway. In addition, raft-activated PDK1 may play other important roles, because PDK1, as the master regulator of AGC kinase signal transduction (5), activates many other critical kinases, including protein kinase C (PKC), ribosomal S6 kinase (S6K), serum and glucocorticoid-inducible kinase (SGK), and p21-activated kinases (PAK). In this vein, one study has shown that raft PDK1 recruits PKC and additional components to assemble a signaling complex that mediates NF-κB signaling in Jurkat cells stimulated with anti-CD3 and anti-CD28 (24).

Future studies should further elucidate the mechanisms of this activation; for example, by examining Y373 phosphorylation, which has been shown to contribute to PV-induced PDK1 activation in the plasma membrane (11). The membrane microdomain-specific dynamics of PI(3,4,5)P_3, which is another component involved in PDK1 activation, have not been systematically characterized. However, several lines of evidence suggest that PI(3,4,5)P_3 may not be exclusively confined in specific membrane microdomains. For example, although PI(3,4,5)P_3 exhibits structural features unfavorable for inclusion into raft microdomains, it has been proposed that the PI(3,4,5)P_3-containing raft microdomains can be formed upon PH domain binding to PI(3,4,5)P_3 (7). Nonetheless, we showed that PI(3,4,5)P_3 production can be detected in nonraft regions (8). Augmentation of this pool of PI(3,4,5)P_3 by overexpression of p110-CAAX, a potentially nonraft-targeted PI3K, can lead to elevated Akt activity (25, 26), possibly involving elevated basal PDK1 activity in nonraft regions.

PTEN is a critical negative regulator of the PI3K/Akt pathway. Our finding that membrane-associated PTEN is preferentially localized to nonraft regions is consistent with previous studies (15, 16), although in some cases raft PTEN has proved undetectable (27), possibly as a result of variations in the cell types and experimental conditions applied. The mechanism underlying this preferential localization to nonraft regions is not clear. One potential mediator is PI(4,5)P_2, a phosphoinositide that is critically involved in the membrane association of PTEN (28, 29). In the absence of protein binding, the polyunsaturated 2'-arach-

idonate chain of $PI(4,5)P_2$ does not favor partitioning into membrane rafts (7). We further showed that the localization of PTEN to nonraft regions is critical to preserving the activity of PI3K/Akt pathway (Fig. 4*A*). Genetic targeting of PTEN A4, an active form of PTEN, to membrane rafts completely abolished the activation of PDK1 in rafts, and membrane recruitment of Akt and its activity. Nonraft-targeted PTEN A4, however, showed inhibitory effects but did not prevent this pathway from being activated. The inhibition by nonraft-targeted PTEN A4 could have resulted from nonspecific effects of overexpressing an active PTEN. However, there is also a possibility that the enzyme molecules, which are localized proximal to membrane rafts, could directly interfere with signaling in raft microdomains.

Based on these findings, we propose a model of membrane microdomain-mediated PI3K/Akt activation (Fig. 4*A*). Both the raft-specific activation of PDK1 and the lack of PTEN-mediated down-regulation in these microdomains are believed to contribute to the preferential activation of Akt in membrane rafts (8). However, our most striking finding was that perturbing this microdomain compartmentalization, either by genetic targeting of active PTEN to rafts or by ceramide-induced translocation of PTEN to the rafts, abolished the activity of the PI3K/Akt pathway. The observed inhibition of Akt recruitment upon raft disruption (7) is in line with this finding. Thus, plasma membrane microdomains can serve as platforms both for concentrating active signaling components such as activated PDK1 and Akt and for segregating them from nonraft-associated negative regulators such as PTEN, thereby enabling the activation and functioning of the PI3K/Akt pathway. From a broader perspective, these data suggest that spatial compartmentalization not only defines the specificity and enhances the efficiency of signal transduction, but it also enables the activation and signaling mediated by critical pathways.

Dysregulation of this compartmentalization may occur under pathological conditions. Ceramide is a lipid metabolite known to induce insulin resistance, and the underlying mechanisms are complex and not well understood (19). For example, ceramide has been shown to recruit the atypical PKC isoform PKCζ to membrane rafts, where PKCζ phosphorylates the PH domain of Akt and blocks its ability to interact with 3′-phosphoinositides (21, 30). However, ceramide has also been shown to promote the dephosphorylation of Akt by activating the Akt phosphatase, protein phosphatase 2A (PP2A), one of the earliest known ceramide targets (31, 32). Here, we propose that the ceramide-induced mislocalization of PTEN to membrane rafts, together with the aforementioned mechanisms, critically contributes to the inhibitory effect of ceramide on PI3K/Akt signaling (Fig. 4*B*). Furthermore, our genetic targeting of PTEN to membrane rafts recapitulated the strong inhibitory effects of ceramide on the activation of PDK1 and Akt. Together, these data suggest that membrane-microdomain compartmentalization is critical for maintaining proper PI3K/Akt signaling in response to insulin, and dysregulating raft-localized PI3K/Akt signaling by recruiting PTEN to these microdomains may be an underlying molecular mechanism for the insulin resistance caused by excess nutrients such as saturated fatty acids.

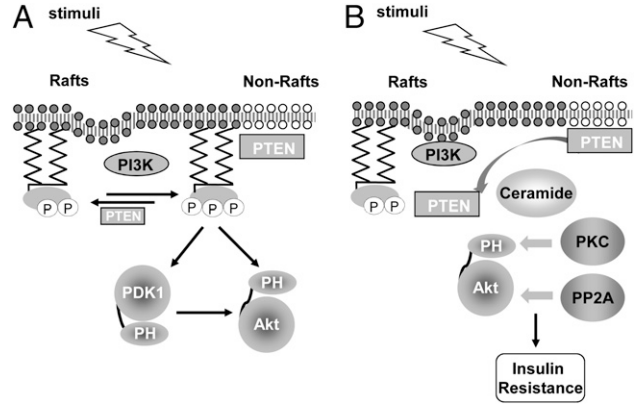

Fig. 4. Compartmentalized PDK1 and PTEN activity in membrane microdomains is essential for proper PI3K/Akt signaling. (*A*) Preferential activation of Akt in membrane rafts is mediated by activated PDK1 in rafts and lack of PTEN-mediated down-regulation in these microdomains. (*B*) Dysregulation of the raft-localized PI3K/Akt signaling as the underlying mechanism for insulin resistance. Ceramide may inhibit Akt signaling through promoting PKCζ phosphorylation of Akt or activating the Akt phosphatase PP2A. The ceramide-induced mislocalization of PTEN to membrane rafts critically contributes to the inhibitory effect of ceramide on PI3K/Akt signaling.

Materials and Methods

Materials. PDGF, EGF, LY294002, MCD, H_2O_2, Na_3VO_4, and C_2-ceramide were purchased from Sigma-Aldrich. Anti-Akt, phospho-Akt (T308), tubulin, and PTEN antibodies were obtained from Cell Signaling Technology, and GFP antibody was from eBioscience. Horseradish peroxidase-conjugated cholera toxin subunit B was purchased from Molecular Probes, catalase was purchased from CalBiochem, and Lipofectamine 2000 was purchased from Invitrogen. Complete Protease Inhibitor Mixture Tablets were obtained from Roche Applied Science.

Preparation of Pervanadate. Pervanadate was prepared as described (33). In brief, 25 μL of 500 mM Na_3VO_4 and 1 μL of 30% (vol/vol) H_2O_2 were mixed in 574 μL of PBS. After 5 min, catalase was added to release excess H_2O_2, which yielded 20 mM pervanadate.

Constructs. PARE was generated by sandwiching full-length PDK1 between a FRET pair, ECFP and citrine. Lyn-PARE and PARE-Kras were generated by the addition of the N-terminal portion of the Lyn kinase gene (GCIKSKRKDKD) at the 5′-end and a CAAX tag at the 3′-end (KKKKKSKTKCVIM) of PARE, respectively. Lyn-ECFP PARE and Lyn Citrine PARE were generated by substituting the fluorescent protein in Lyn-PARE with ECFP or citrine, respectively. Lyn-PARE R472/474A was generated by site-directed mutagenesis. PTEN A4 (fused with a C-terminal fluorescent protein) was targeted to raft and nonraft regions of the plasma membrane with the same set of targeting motifs. All of the constructs were generated in a modified version of the mammalian expression vector pcDNA 3.

Cell Transfection and Imaging. Cells were plated on sterilized glass coverslips in 35-mm dishes and were grown to 40% confluency in medium at 37 °C with 5% CO_2, then transfected with Lipofectamine 2000. In the case of NIH 3T3 and HeLa cells, the cells were serum-starved for 24 h. For imaging, cells were washed with Hanks' balanced salt solution (HBSS) and imaged in the dark at room temperature. Images were acquired on a Zeiss Axiovert 200M microscope with a cooled charge-coupled device camera, as described (8). Dual-emission ratio imaging was performed with a 420DF20 excitation filter, a 450DRLP dichroic mirror, and two emission filters. For CFP and YFP, 475DF40 and 535DF25, respectively, were used. Exposure times were 50–500 ms. Images were taken every 30 s. Imaging data were analyzed with Metafluor 6.2 software (Universal Imaging). Fluorescence images were background-corrected by deducting the background (from regions with no cells) from the emission intensities of CFP or YFP. Regions of interest at the cell periphery representing the plasma membrane were used for analysis for Lyn-PARE and PARE-Kras. Traces were normalized by taking the emission ratio before addition of drugs as 1.

Western Blot Analysis. Cells were washed with ice-cold PBS and then lysed in RIPA lysis buffer containing protease inhibitor mixture, 1 mM PMSF, 1 mM Na_3VO_4, 1 mM NaF, and 25 nM calyculin A. Total cell lysates were incubated on ice for 30 min, then centrifuged at 4 °C for 20 min. Total protein was separated with 7.5% SDS/PAGE and transferred to nitrocellulose membranes. The membranes were blocked with TBS containing 0.05% Tween-20 and 1% BSA and then incubated with primary antibodies overnight at 4 °C. After incubation with the appropriate horseradish peroxidase-conjugated secondary antibodies, the bands were visualized by enhanced chemiluminescence. The intensity of the bands was quantified with ImageJ software.

Membrane Preparation. Cells were rinsed twice with ice-cold PBS and harvested into 10 mM Tris (pH 7.4) with 150 mM NaCl, 5 mM EDTA, 2 mM PMSF, 2 mM Na_3VO_4, 2 mM NaF, and 50 nM calyculin A, with protease inhibitor mixture. The cells then were subjected to mechanical disruption with 15 strokes of a homogenizer. Homogenates were centrifuged at 2,300 × *g* for 5 min at 4 °C, and the supernatant was centrifuged at 18,000 × *g* for 50 min at 4 °C (34). The resulting membrane pellets were resuspended in 10 mM Tris (pH 7.4) with 150 mM NaCl, 5 mM EDTA, 2 mM PMSF, 2 mM $NaVO_4$, 2 mM NaF, and 50 nM calyculin A, with protease inhibitor mixture and 1% Triton X-100, for sucrose density gradient fractionation.

Sucrose Density Gradient Fractionation. Crude plasma membranes (or total cell lysates) were incubated in ice with periodic mixing for 1 h, then diluted 1:1 with 80% sucrose and layered on 4 mL of 35% sucrose, followed by the addition of 1 mL of 5% sucrose solution and 4.5 mL of 10 mM Tris (pH 7.4) containing 150 mM NaCl and 5 mM EDTA. Ultracentrifugation was performed at 39,000 × *g* for 18 h in a Beckman SW41-Ti rotor. All experimental steps were performed at 4 °C. After ultracentrifugation, the top 3.5 mL of the sample was discarded. Nine 880-μL fractions were then collected, starting from the top of the gradient. The fractions were dot-blotted on nitrocellulose membranes and probed with HRP-conjugated cholera toxin subunit B antibody to identify the raft-containing fractions.

Differentiation of 3T3-L1 Adipocytes. 3T3-L1 preadipocytes were grown to confluency in 10% calf serum/DMEM and stimulated with induction media (DMEM containing 10% FBS, 1 μg/mL insulin, 1 μM dexamethasone, and 0.5 mM 3-isobutyl-L-methylxanthine) at 2 d after confluency. The medium was changed to insulin medium (1 μg/mL) 2 d after induction. Two days later, the medium was replaced with 10% FBS/DMEM and then changed every 2 d. Full differentiation was achieved by 8 d after induction.

Glucose Uptake Assay. Adipocytes were incubated in Krebs–Ringer bicarbonate buffer supplemented with 30 mM Hepes at pH 7.4, with 0.5% BSA and 2.5 mM glucose for 3 h. The cells were washed once with PBS and incubated in BSA/KRH [25 mM Hepes-NaOH (pH 7.4), with 120 mM NaCl, 5 mM KCl, 1.2 mM $MgSO_4$, 1.3 mM $CaCl_2$, and 1.3 mM KH_2PO_4] without glucose for 15 min. The cells were then incubated with 100 nM insulin for 15 min. The assay was initiated by the addition of [^{14}C]2-deoxyglucose (0.4 μCi per sample) and 5 mM glucose and terminated after 15 min by washing the cells three times with ice-cold PBS. Cells were solubilized in 1% Triton X-100, and cell-associated radioactivity was determined by scintillation counting.

ACKNOWLEDGMENTS. We thank Qiang Ni for critical reading of the manuscript and Deborah Ann McClellan for editorial assistance. This work was supported by National Institutes of Health (NIH) Grants R01 DK-073368 and R21 CA-122673 (to J. Z.). C.D. is supported by NIH Predoctoral Fellowship F31 GM087079. Z.W. is supported by American Heart Association Predoctoral Fellowship PRE3790034. G.W.W. is supported by American Heart Association Grant SDG2260721, Baltimore Diabetes Research and Training Center Grant (P60DK079637), and NIH Grant DK084171.

1. Franke TF (2008) PI3K/Akt: Getting it right matters. *Oncogene* 27:6473–6488.
2. Wong KK, Engelman JA, Cantley LC (2010) Targeting the PI3K signaling pathway in cancer. *Curr Opin Genet Dev* 20:87–90.
3. Farese RV, Sajan MP, Standaert ML (2005) Insulin-sensitive protein kinases (atypical protein kinase C and protein kinase B/Akt): Actions and defects in obesity and type II diabetes. *Exp Biol Med (Maywood)* 230:593–605.
4. Bozulic L, Hemmings BA (2009) PIKKing on PKB: Regulation of PKB activity by phosphorylation. *Curr Opin Cell Biol* 21:256–261.
5. Mora A, Komander D, van Aalten DM, Alessi DR (2004) PDK1, the master regulator of AGC kinase signal transduction. *Semin Cell Dev Biol* 15:161–170.
6. Simons K, Toomre D (2000) Lipid rafts and signal transduction. *Nat Rev Mol Cell Biol* 1: 31–39.
7. Lasserre R, et al. (2008) Raft nanodomains contribute to Akt/PKB plasma membrane recruitment and activation. *Nat Chem Biol* 4:538–547.
8. Gao X, Zhang J (2008) Spatiotemporal analysis of differential Akt regulation in plasma membrane microdomains. *Mol Biol Cell* 19:4366–4373.
9. Hoeller D, Volarevic S, Dikic I (2005) Compartmentalization of growth factor receptor signalling. *Curr Opin Cell Biol* 17:107–111.
10. Casamayor A, Morrice NA, Alessi DR (1999) Phosphorylation of Ser-241 is essential for the activity of 3-phosphoinositide-dependent protein kinase-1: Identification of five sites of phosphorylation in vivo. *Biochem J* 342:287–292.
11. Park J, et al. (2001) Identification of tyrosine phosphorylation sites on 3-phosphoinositide-dependent protein kinase-1 and their role in regulating kinase activity. *J Biol Chem* 276:37459–37471.
12. Bayascas JR, et al. (2008) Mutation of the PDK1 PH domain inhibits protein kinase B/Akt, leading to small size and insulin resistance. *Mol Cell Biol* 28:3258–3272.
13. Komander D, et al. (2004) Structural insights into the regulation of PDK1 by phosphoinositides and inositol phosphates. *EMBO J* 23:3918–3928.
14. Tamguney T, Stokoe D (2007) New insights into PTEN. *J Cell Sci* 120:4071–4079.
15. Caselli A, Mazzinghi B, Camici G, Manao G, Ramponi G (2002) Some protein tyrosine phosphatases target in part to lipid rafts and interact with caveolin-1. *Biochem Biophys Res Commun* 296:692–697.
16. Jahn T, Leifheit E, Gooch S, Sindhu S, Weinberg K (2007) Lipid rafts are required for Kit survival and proliferation signals. *Blood* 110:1739–1747.
17. Vazquez F, Ramaswamy S, Nakamura N, Sellers WR (2000) Phosphorylation of the PTEN tail regulates protein stability and function. *Mol Cell Biol* 20:5010–5018.
18. Lee SR, et al. (2002) Reversible inactivation of the tumor suppressor PTEN by H_2O_2. *J Biol Chem* 277:20336–20342.
19. Holland WL, Summers SA (2008) Sphingolipids, insulin resistance, and metabolic disease: New insights from in vivo manipulation of sphingolipid metabolism. *Endocr Rev* 29:381–402.
20. Goswami R, Singh D, Phillips G, Kilkus J, Dawson G (2005) Ceramide regulation of the tumor suppressor phosphatase PTEN in rafts isolated from neurotumor cell lines. *J Neurosci Res* 81:541–550.
21. Hajduch E, et al. (2008) Targeting of PKCzeta and PKB to caveolin-enriched microdomains represents a crucial step underpinning the disruption in PKB-directed signalling by ceramide. *Biochem J* 410:369–379.
22. Summers SA, Garza LA, Zhou HL, Birnbaum MJ (1998) Regulation of insulin-stimulated glucose transporter GLUT4 translocation and Akt kinase activity by ceramide. *Mol Cell Biol* 18:5457–5464.
23. Masters TA, et al. (2010) Regulation of 3-phosphoinositide-dependent protein kinase 1 activity by homodimerization in live cells. *Sci Signal* 3:ra78.
24. Lee KY, D'Acquisto F, Hayden MS, Shim JH, Ghosh S (2005) PDK1 nucleates T cell receptor-induced signaling complex for NF-kappaB activation. *Science* 308:114–118.
25. Egawa K, et al. (1999) Membrane-targeted phosphatidylinositol 3-kinase mimics insulin actions and induces a state of cellular insulin resistance. *J Biol Chem* 274: 14306–14314.
26. Takano A, et al. (2001) Growth hormone induces cellular insulin resistance by uncoupling phosphatidylinositol 3-kinase and its downstream signals in 3T3-L1 adipocytes. *Diabetes* 50:1891–1900.
27. Odriozola L, Singh G, Hoang T, Chan AM (2007) Regulation of PTEN activity by its carboxyl-terminal autoinhibitory domain. *J Biol Chem* 282:23306–23315.
28. Walker SM, Leslie NR, Perera NM, Batty IH, Downes CP (2004) The tumour-suppressor function of PTEN requires an N-terminal lipid-binding motif. *Biochem J* 379:301–307.
29. Iijima M, Devreotes P (2002) Tumor suppressor PTEN mediates sensing of chemoattractant gradients. *Cell* 109:599–610.
30. Powell DJ, Hajduch E, Kular G, Hundal HS (2003) Ceramide disables 3-phosphoinositide binding to the pleckstrin homology domain of protein kinase B (PKB)/Akt by a PKCzeta-dependent mechanism. *Mol Cell Biol* 23:7794–7808.
31. Chavez JA, et al. (2003) A role for ceramide, but not diacylglycerol, in the antagonism of insulin signal transduction by saturated fatty acids. *J Biol Chem* 278:10297–10303.
32. Dobrowsky RT, Kamibayashi C, Mumby MC, Hannun YA (1993) Ceramide activates heterotrimeric protein phosphatase 2A. *J Biol Chem* 268:15523–15530.
33. Huyer G, et al. (1997) Mechanism of inhibition of protein-tyrosine phosphatases by vanadate and pervanadate. *J Biol Chem* 272:843–851.
34. Pontier SM, et al. (2008) Cholesterol-dependent separation of the beta2-adrenergic receptor from its partners determines signaling efficacy: Insight into nanoscale organization of signal transduction. *J Biol Chem* 283:24659–24672.